Supplement

The supplement presents details regarding 1-the acquisition and processing of the DEM shown in Figure 2, 2- the meteorological data from the local station in Qatar, 3-the sand grain distribution analysis, and 4-the drift potential analysis.

Drone flight details

We used a drone (DJI Phantom 3 professional) and the structure from motion technique to generate a high quality DEM (Figure 2). The acquisition of the pictures was done using the Point of Interest flight mode where the aircraft continuously circle around a selected coordinate, respectively the center of the dune for our study. The flight was carried around 4pm, local hour. Four flights were needed for battery reason, each lasting around 15 minutes. Over 300 photos were taken at different angles around the dune and at different elevation. We used then the AGISOFT software to calculate the DEM. The alignment of photos accuracy parameter was set to high and the density of the point cloud generated was fixed to medium for computational reason. The software then produces a DEM from this point cloud, interpolating between the points. The end-product is a meshgrid with a ground sampling distance of ~0.6m and vertical accuracy depending on the density of common points found by the software between the pictures. We found that the upper portion of the dune seems reasonably defined whereas the lower part had a stronger bias (slight depression in the DEM that should not be present) because of the fewer common points found by the software due to the slick surface of this dune's section.

Mast rotation and data gap bias

The mast of the installation has been rotating gradually to the West throughout the years. This shift in azimuth is assumed linear in time and the wind direction has been consequently corrected for it (Figure S1). Additionally, a bit more than one day of data is missing between those 2 years. Considering the total

681   amount of data, this void will have in the end a minimal impact on the calculation of Q_s, especially since

682   almost all of it happened during the calm spring season.

Sand grain distribution

684   Each grain size sample collected from the field was split in half four times using a grain sample splitter to

685   ensure that no bias was introduced during grain size measurement. Grain size distributions were

686   measured using a Retsch-Camsizer. The Camsizer digitally imaged millions of particles per sample and

687   grain size distributions were generated from the nominal grain diameters measured from 19

688   logarithmically-spaced size classes between 0.04-0.85 mm. Diameter is measured by the Camsizer as the

689   shortest axis in a planar projection, which is equivalent to the intermediate axis of a 3d particle shape.

690   The results are shown in Figure S2 and Table S1.
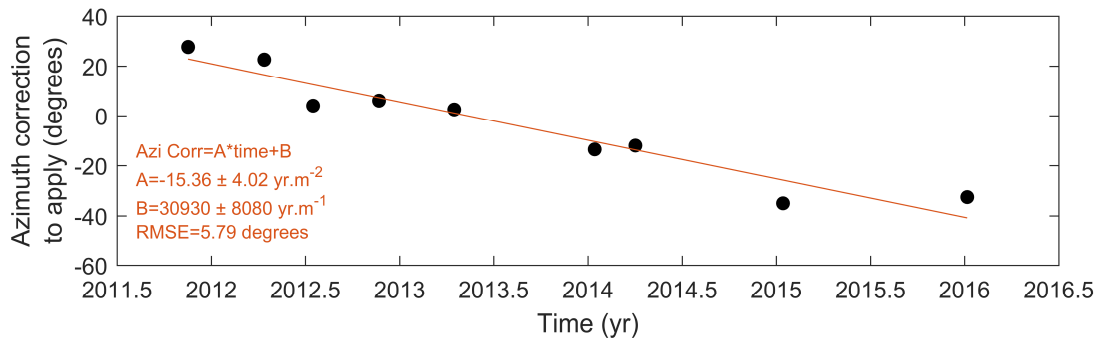
Drift Potential analysis

692   The Drift Potential (DP), the resultant DP (RDP), RDP/DP and Resultant Drift Direction (RDD) (Fryberger,

693   1979) have been calculated using $u_{*t} = 0.261$ m/s (value using $Dp = 236\,\mu$ m and Equation (7) in the

694   main text) (Figure S3). Those estimates are for wind at 10m height. We observe that longer time averaging

695   diminishes RDP and DP, which is a direct consequence of the increasing dilution of strong winds. Going

696   from 1-minute to 6-hour averages, the RDP/DP increases from 0.87 to 0.92, indicating a dilution of the

697   direction variability of the wind as the time window averaging is increased. The RDP/DP is for all cases

698   very high, stressing the mono-directionality of Qatar winds.

699
700
Bibliography

Fryberger, S.G. and Dean, G., 1979. Dune forms and wind regime. In *A study of global sand seas* (Vol.

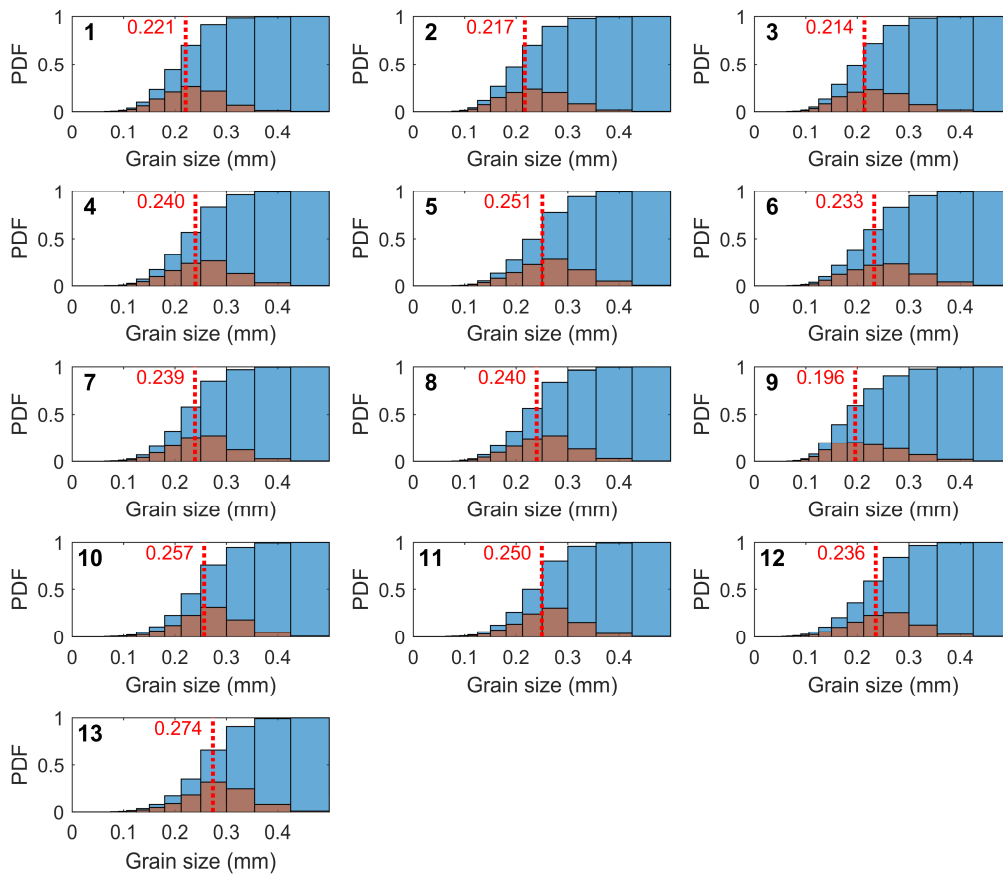   1052, pp. 137-169). US Government Printing Office Washington.

701

702

703 *Figure S1. Azimuth drift of the mast. The black dots indicate the measured mast azimuth correction needed at those date. The*

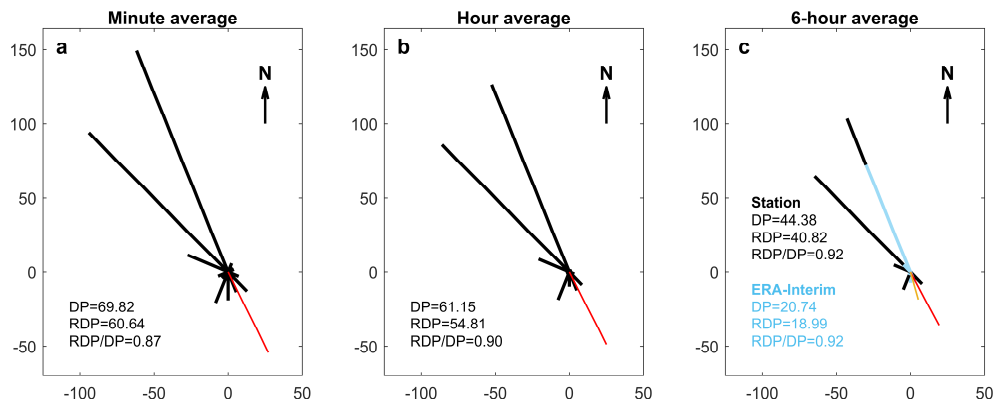704 *orange line is the linear fit of those measurements.*

705

706

Figure S2. Particle size histograms for each samples indicated in Figure 2. Samples (which numbers are indicated in black in this figure) are located from NW (sample 1) to SE (sample 13). The orange histograms represent the Probability Density Function (PDF) of the grain size distribution. The blue histograms represent the cumulative PDF of grain size distribution. The red dotted lines, and their associated red number, indicate the median grain size.

707

708

709

710

711

712

Minute average	Hour average	6-hour average

a
N

DP=69.82
RDP=60.64
RDP/DP=0.87

b
N

DP=61.15
RDP=54.81
RDP/DP=0.90

c
N

Station
DP=44.38
RDP=40.82
RDP/DP=0.92

ERA-Interim
DP=20.74
RDP=18.99
RDP/DP=0.92

713

714 *Figure S3. Drift potential (DP) analysis for each time average (in m^3/s^3). Black lines correspond to the DP rose of the*

715 *meteorological station. Red lines indicate the resultant drift direction (RDD) of the meteorological station. Blue lines in (c)*

716 *indicate the DP rose of ERA-Interim. The yellow line indicates its resultant drift direction (RDD).*

717

718

719

720   *Table S1. Grain size distribution analysis of the 13 sand samples. Their location is indicated in Figure 2, going from sample 1 in*

721   *the NW to sample 13 to the SE.*

Sample	d50	d90	d10	grain size Wentworth-scale adjetival classificiation	Sorting (Folk and Ward (1957), Phi)	sorting adjetival classification
1	0.221	0.294	0.15	fine	0.374	well sorted
2	0.217	0.301	0.145	fine	0.398	well sorted
3	0.214	0.297	0.142	fine	0.400	well sorted
4	0.24	0.322	0.16	fine	0.372	well sorted
5	0.251	0.334	0.17	medium	0.357	well sorted
6	0.233	0.327	0.141	fine	0.403	well sorted
7	0.239	0.315	0.163	fine	0.355	well sorted
8	0.24	0.319	0.162	fine	0.364	well sorted
9	0.196	0.297	0.131	fine	0.425	well sorted
10	0.257	0.334	0.178	medium	0.341	very well sorted
11	0.25	0.325	0.172	medium	0.343	very well sorted
12	0.236	0.317	0.148	fine	0.393	well sorted
13	0.274	0.351	0.189	medium	0.345	very well sorted

722